journal

Ultrasonic Dispersion of TiO$_2$ Nanoparticles in Aqueous Suspension

Kimitoshi Sato,[‡] Ji-Guang Li,[‡] Hidehiro Kamiya,*,[§] and Takamasa Ishigaki*,[†,‡]

[‡]Nano Ceramics Center, National Institute for Materials Science, Ibaraki 305-0044, Japan

[§]Tokyo University of Agriculture and Technology, BASE, Tokyo 184-8588, Japan

Aggregation and dispersion behavior of nanometer and submicrometer scale TiO$_2$ particles in aqueous suspension were investigated using three kinds of mechanical dispersion methods: ultrasonic irradiation, milling with 5-mm-diameter balls, and milling with 50 μm beads. Polyacrylic acids with molecular weights ranging from 1200 to 30 000 g/mol were used as a dispersant, and the molecular weight for each dispersion condition was optimized. Viscosities and aggregate sizes of the submicrometer powder suspensions were not appreciably changed in the ultrasonic irradiation and 5-mm-ball milling trials. In contrast, in the trials in which nanoparticle suspension was used, ultrasonic irradiation produced better results than 5-mm-ball milling. Use of ultrasonication enabled dispersion of aggregates to primary particle sizes, which was determined based on the specific surface area of the starting TiO$_2$ powders, even for relatively high solid content suspensions of up to 15 vol%. Fifty-micrometer-bead milling was also able to disperse aggregates to the same sizes as the ultrasonic irradiation method, but 50-μm-bead milling can be used only in relatively low solid content suspensions. It was concluded that the ultrasonic dispersion method was a useful way to prepare concentrated and highly dispersed nanoparticle suspensions.

I. Introduction

TITANIUM dioxide nanoparticles are used for a wide range of applications such as in photocatalysts,[1] photovoltaic cells,[2] batteries,[3] photochromic and electrochromic devices,[4] and gas sensors.[5] Submicrometer- and micrometer-sized coarse TiO$_2$ powders have been commercially produced by the so-called sulfate and chloride processes, in which titanyl sulfate or titanium chloride is formed from titanium ores and is then oxidized by heating in oxygen. TiO$_2$ nanopowders have been produced on an industrial scale by flame oxidation of titanium tetrachloride and related reactants[6] and by a sol–gel process.[7] Controlling the dispersion and aggregation of the nanoparticles in suspension is crucial to exploiting the advantages of nanoparticles. One useful process is simultaneous synthesis and dispersion, which yields a well-dispersed nanoparticle suspension, for example, a reverse micelle technique,[8] which can simultaneously synthesize and disperse TiO$_2$ nanoparticles in the solvent. However, this technique has drawbacks with regard to production, namely, reaggregation during the micelle removal process and a low solid fraction in the suspension. Therefore, the development of surface modification techniques that use dispersants and physical dispersion technology to achieve well-dispersed nanoparticle suspensions with high solid fractions would greatly advance the industrial use of nanoparticles.

Polyacrylic acids are effective as dispersants for oxides, such as Al$_2$O$_3$ and TiO$_2$.[9,10] It is known that, because of the enhanced steric effect, concentrated suspensions have low viscosity when the adsorbed dispersants form a loop and train structure, while high viscosity is observed when a flat structure is formed by the adsorbed dispersant.[9]

Nanopowders agglomerate more strongly than submicrometer powders, and some of the particles coagulate strongly. Agglomerated nanoparticles do not fragment easily and are difficult to disperse perfectly using millimeter-sized ball milling. Therefore, physical and mechanical dispersion methods are needed to disperse nanoparticles perfectly.

Bead milling with balls several tens of micrometers in diameter has recently been developed as a new method to disperse nanoparticles to almost primary particle size.[11] However, it is difficult to work with slurries with high solid fractions using the bead milling. We focused on ultrasonic irradiation as the method of dispersing nanoparticles to primary particle size even with high solid fraction slurries.

Ultrasonic irradiation into suspensions of submicrometer-sized particles is an effective tool for eliminating agglomeration, and the relationship between irradiation conditions and measured particle size has been studied.[12,13] Ultrasonic irradiation generates shock waves by collapsing cavitations, which then leads to collisions among particles. The agglomerated particles are thus eroded and split by the collisions.[14–17] A report has recently been made on the effect of ultrasonic irradiation on the slurry viscosity, sintered density, and properties of the resultant ceramics.[18,19] However, the effects of ultrasonication on nanoparticle dispersion have not been systematically investigated.

The present study focuses on the effects of ultrasonic irradiation on slurry viscosity and aggregate size of nanocrystalline TiO$_2$ aqueous suspensions containing polymer dispersants. The results are compared with those obtained via 5-mm-ball milling and 50-μm-bead milling.

II. Experimental Procedure

(1) Starting Materials

Three kinds of TiO$_2$ powders were used in this work: nanoparticulate P25 (Nippon Aerosil Co. Ltd., Tokyo, Japan), nanoparticulate ST21 (Ishihara Sangyo Kaisya Ltd., Osaka, Japan), and submicrometer HT0514 (Toho Titanium Co. Ltd., Chigasaki, Japan). P25 and HT0514 were manufactured by vapor phase synthesis; ST21 was manufactured by a wet-chemical synthesis. Figure 1 shows scanning electron microscopic (SEM) images of the TiO$_2$ nanopowders (P25 and ST21) and the submicrometer powder (HT0514). The images were obtained using a scanning electronic microscope (model S-5000, Hitachi, Tokyo, Japan) after the TiO$_2$ particles were ultrasonically dispersed in distilled water for 5 min, after which several drops of the sample suspension were dried on the SEM sample stage. Both nanopowders formed aggregates. The primary particles of each powder had a narrow size distribution. Specific surface areas as determined by a BET method (BELSORP18, Bell Japan Inc., Osaka, Japan) after pretreatment at 200°C under 10^{-2} torr for 50 min are 46.5, 63.5, and 5.8 m^2/g for P25, ST21, and
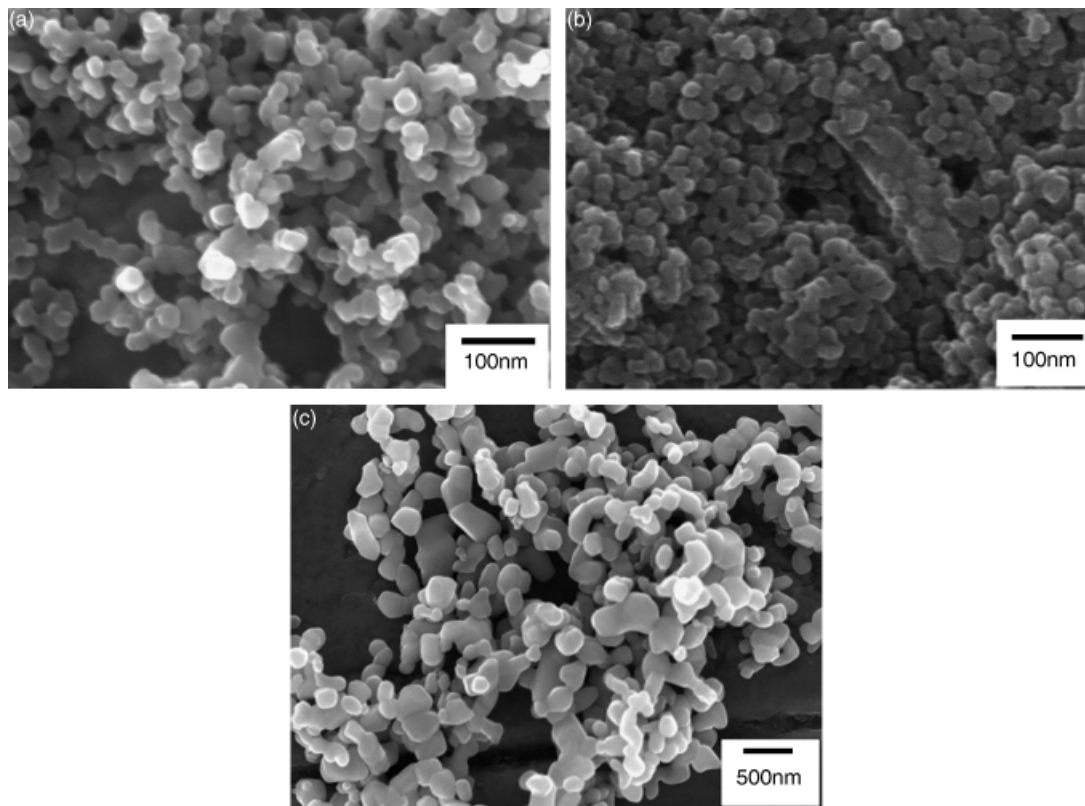
Fig. 1. Scanning electron micrograph of commercial TiO_2 powders. (a) P25 (46.5 m^2/g); (b) ST21 (63.5 m^2/g); and (c) HT0514 (5.8 m^2/g, submicrometer powder).

HT0514, respectively. Densities of the nanoparticulate and submicrometer particles measured by the suppliers using pycnometers are 3.7, 3.7, and 4.0 g/cm^3 for P25, ST21, and HT0514, respectively. Primary particle size distribution was determined from an image analysis of SEM images in which 1000 particles were counted. Mean primary particle size of the powders was also estimated based on the specific surface area and powder density data. Degree of dispersion was evaluated by comparing the measured particle size, i.e., aggregate cluster size, in suspension with the primary particle size. X-ray diffraction studies showed that the P25 nanopowder is composed of a mixture of anatase (~ 70%) and rutile (~ 30%), ST21 nanopowder is anatase phase, and HT0514 submicrometer-sized powders are rutile phase.

(2) Suspension Preparation

Sodium polyacrylates (PAA) with average molecular weights of 1200, 2100, 8000, 15 000, and 30 000 (Sigma-Aldrich Corp., St. Louis, MO) were used as a polymer dispersant. To prepare aqueous suspensions, the TiO_2 powders were mixed with PAA in water. pH was adjusted with ammonia solution (20%, analytical grade, Wako Pure Industries Ltd., Osaka, Japan). Three kinds of dispersion techniques were used in this work: ultrasonication, bead milling with 50 μm ZrO_2 beads (PCM-LR, net volume 50 mL; Asada Iron Works Co. Ltd., Osaka, Japan), and ball milling with 5 mm Al_2O_3 balls. The solid fractions were fixed at 15 vol% for ultrasonication and ball milling, and at 1 vol% for 50 μm ZrO_2 bead milling because the 50 μm ZrO_2 beads cannot be separated by the centrifugal force and filter screen method at solid fractions as high as 15 vol%. The amount of PAA added was 0.5 mg per unit particle surface area (m^2), and the pH was 8.5 for all the suspensions.

For ultrasonication, a 50 mL suspension was ultrasonically irradiated in a 100-mL beaker for 30 min. To prevent the water from boiling and the PAA from gelling, the suspension was irradiated ten times for 3 min each because 3-min continuous irradiation leads to a 60°–70°C increase in temperature. After

each 3-min continuous irradiation, the suspension was cooled for 10 min. We used two kinds of ultrasonic generators, a UT300 (Nihon Seiki Kaisha Ltd., Tokyo, Japan; frequency: 20 kHz; vibration amplitude: 30–34 μm; generating power: 70–120 W; probe diameter: 26 mm) and an SMT600 (SMT Ltd., Tokyo, Japan; frequency: 20 kHz; vibration amplitude: 40 μm; generating power: 600 W; probe diameter: 36 mm). After a 30-min ultrasonication, the water had decreased by about 10 ml due to evaporation. Therefore, the weight was measured before and after ultrasonication, and pure water was added to compensate for the loss. Also, a decrease of up to 0.5 vol% of the solid fraction of the suspension, which influences viscosity and particle size distribution, was observed after ultrasonication, as the particles adhered to the probe of the ultrasonic homogenizer. Nonetheless, hereafter the stated solid fraction refers to the value before ultrasonication. For example, even though the solid fraction of the slurry decreased from 15 to 14.5 vol%, the solid fraction will hereafter be stated as 15 vol%.

The milling beads used in this study were annular-type PCM-LR (Asada Iron Works Co. Ltd.). A schematic of the bead mill is shown in Fig. 2. The beads were moved by the rotation of a rotator in the opening of a double cylinder, which consisted of a filter screen and a rotator with projections. Beads were disposed of outside an opening during high-speed rotation using centrifugal force. The slurry and beads were separated by a filter screen inside the opening. The vessel was equipped with a water jacket for cooling. Pressure inside the mill chamber was controlled using a safety control device. The appearance packing density of beads in the mill was fixed at 80 vol% for all experimental conditions. The circumferential velocities of agitation were set at 4 and 8 m/s. The circulation rate of slurry was set at 1.7 mL/s. The slurry and PAA of 8000 g/mol in molecular weights were mixed at 300 rpm for 1 h by a mechanical stirrer as a pretreatment for bead milling. During the milling tests, each of which lasted 3 h, 550 mL of TiO_2 slurry passed through the mill and then returned to the mixing tank. Every 30 min, 50 mL of the bead-milled suspension was taken to measure the particle size distribution. There were a total of 45 passes in 3 h.
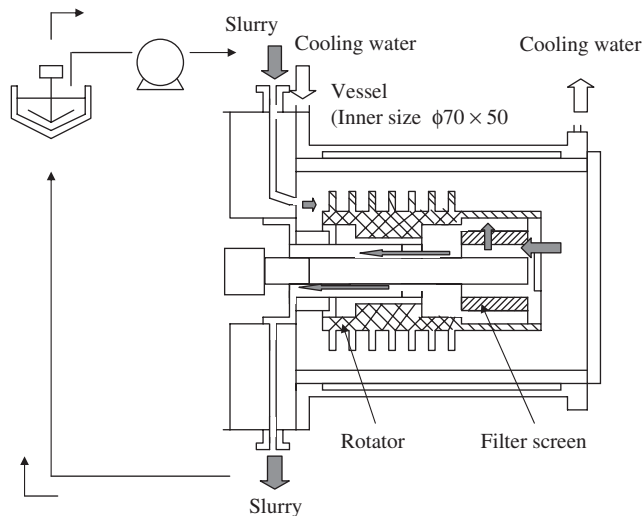
Fig. 2. Schematic of the bead mill.

To prepare suspension for ball milling with 5-mm-diameter alumina balls, the balls were packed into a 300-mL polyethylene bottle with an appearance packing density of 20 vol%. Fifty milliliter of ball-milled suspension was prepared by mixing 15 vol% powder, pure water, and PAA of 8000 g/mol for 24 h at a rotation rate of 60 rpm.

(3) Characterization of the Suspension

The zeta potential of the suspension was measured at various pH values by a model 502 analyzer (Nihon Rufuto Co. Ltd., Tokyo, Japan) after ultrasonication for 5 min. A flow curve of the obtained suspension was measured at 25°C by a concentric double-cylinder viscometer (HAKKE Viscometer VT550, Thermo Electron Gmbh, Karlsruhe, Germany) at a shear rate increasing from 1 to 300 s^{-1} in 90 s and subsequently decreasing at the same rate. The apparent viscosity was measured at the shear rate of 300 s^{-1}.

Aggregate size distribution in the slurry was determined by two methods. An X-ray particle analyzer (BI-XDC, Nikkiso Co. Ltd., Tokyo, Japan) was used for the low solid fraction (1 vol%). The 15 vol% suspension was diluted to 1 vol% by adding pure water, and the particle size in the 1 vol% suspension was measured. For the 15 vol% suspension, the particle size was measured by an ultrasonic attenuation spectrometer (DT1200, Nihon Rufuto Co. Ltd.). No appreciable difference was observed between the values measured by the DT1200 for the 15 vol% suspension and by the BI-XDC for 1 vol% suspension originated from the same 15 vol% suspension.

III. Results and Discussion

(1) Adsorption Condition of PAA on TiO₂ Particles

Figure 3 shows the effects of the additive content of PAA (8000 g/mol) and slurry pH on the flow curve of P25. These suspensions were prepared by 5-mm-ball milling for 24 h. At the same pH condition of 8.5, the optimum additive concentration of PAA to obtain the minimum viscosity was 0.5 mg per unit nanoparticle surface area. When pH was increased from 8.5 to 9.5 at the same PAA content of 0.5 mg, the viscosity of the suspension increased tremendously. Based on these results, the amount of added PAA and suspension pH were fixed at 0.5 mg/m² and 8.5, respectively. Figure 4 shows the variation in zeta potential of the two TiO₂ nanopowders in the pH range from 4 to 10. The isoelectric points (pH$_{IEP}$) of both particles were in the range of pH 6–7. The values of pH$_{IEP}$ of TiO₂ particles were in the same range in previous reports.[20,21] The pH$_{IEP}$ of P25 was higher than that of ST21. This means that the particle surface is negatively charged at pH = 8.5, and the absolute value of surface charge of ST21 is higher than that of P25. The carboxylic
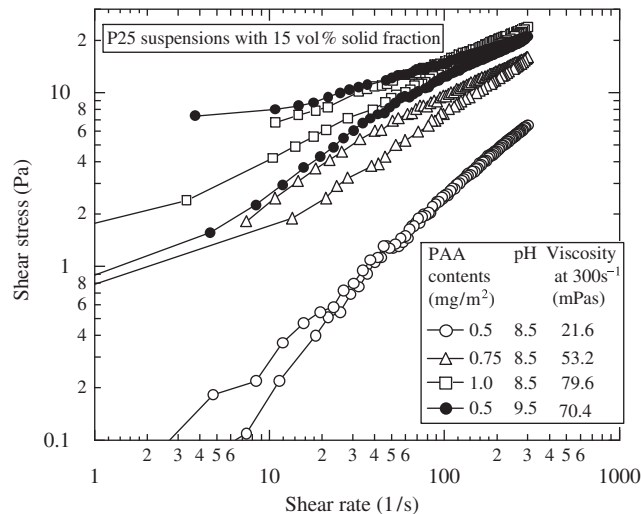

Fig. 3. Flow curve of TiO₂ nanoparticles (P25) suspension as functions of PAA contents and pH. Solid fraction is 15 vol%. The PAA of 8000 g/mol in molecular weight was used.

acid group of PAA dissociated perfectly at pH = 8.5[11]; hence, the carboxylic acid group could be adsorbed on the neutrally charged part of P25 particle surfaces. Because the absolute value of the negative charge on P25 particles was increased by the increase of pH from 8.5 to 9.5, PAA could not be adsorbed on the particle surface and suspension viscosity increased.

(2) Effect of Ultrasonic Irradiation on Dispersion

To determine the ultrasonic irradiation time, its effect on suspension viscosity and size distribution of aggregates in suspension was examined using P25 TiO₂ nanoparticles and is shown in Figs. 5 and 6. These figures show the effects of vibration and probe diameter on ultrasonic irradiation using two kinds of generators: UT300 (Fig. 5, vibration 30–34 μm, frequency 20 kHz, probe diameter 26 mm) and SMT600 (Fig. 6, vibration 40 μm, frequency 20 kHz, probe diameter 36 mm). Regardless of the amplitude of vibration and the size of the probe diameter, the viscosity and mean size of the aggregates in suspension decreased as irradiation time increased. Because the estimated primary particle size from specific surface area is about 35 nm, large aggregates were dispersed almost completely by ultrasonic irradiation for 30 min. The viscosity and aggregate size of the suspension made by the SMT600 at a vibration of 40 μm and probe diameter of 36 mm decreased faster than did those made by the UT300 at a vibration of 30–34 μm and a probe diameter of 26 mm. After ultrasonic irradiation for 30 min, however, the ultrasonication by the two generators resulted in almost the same viscosity and aggregate size.
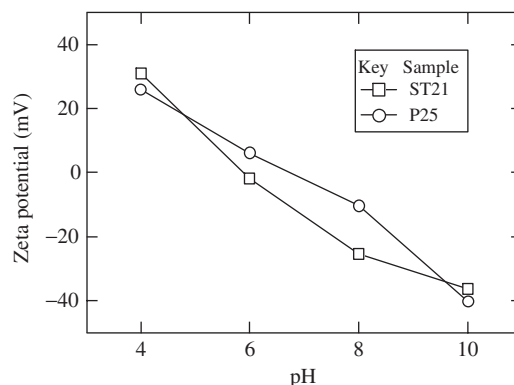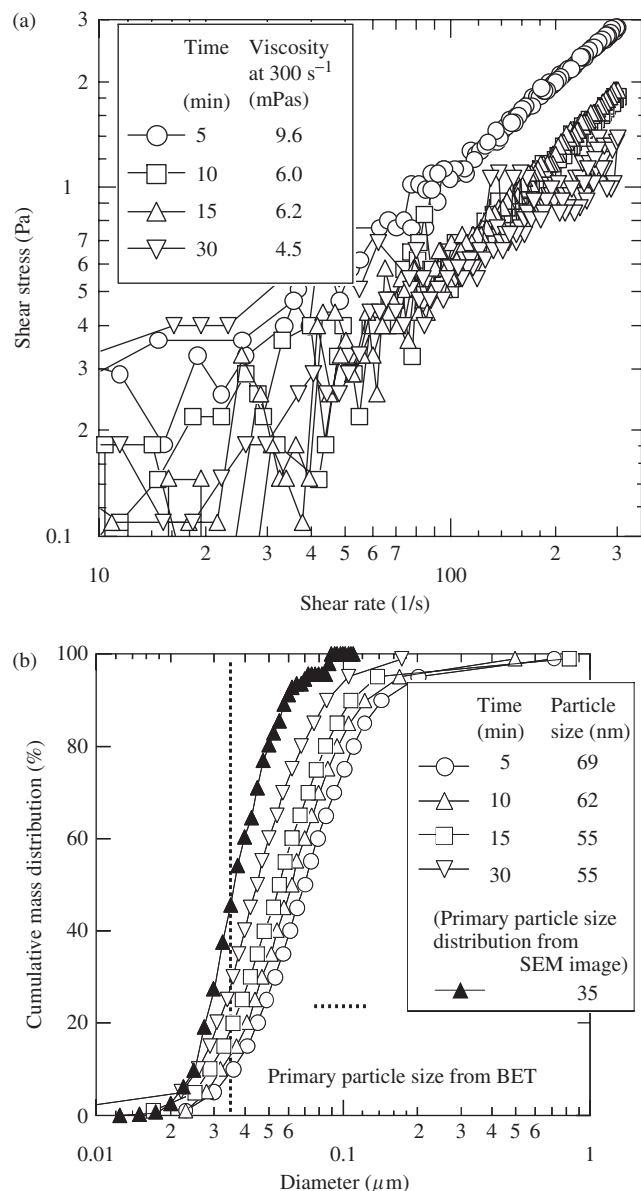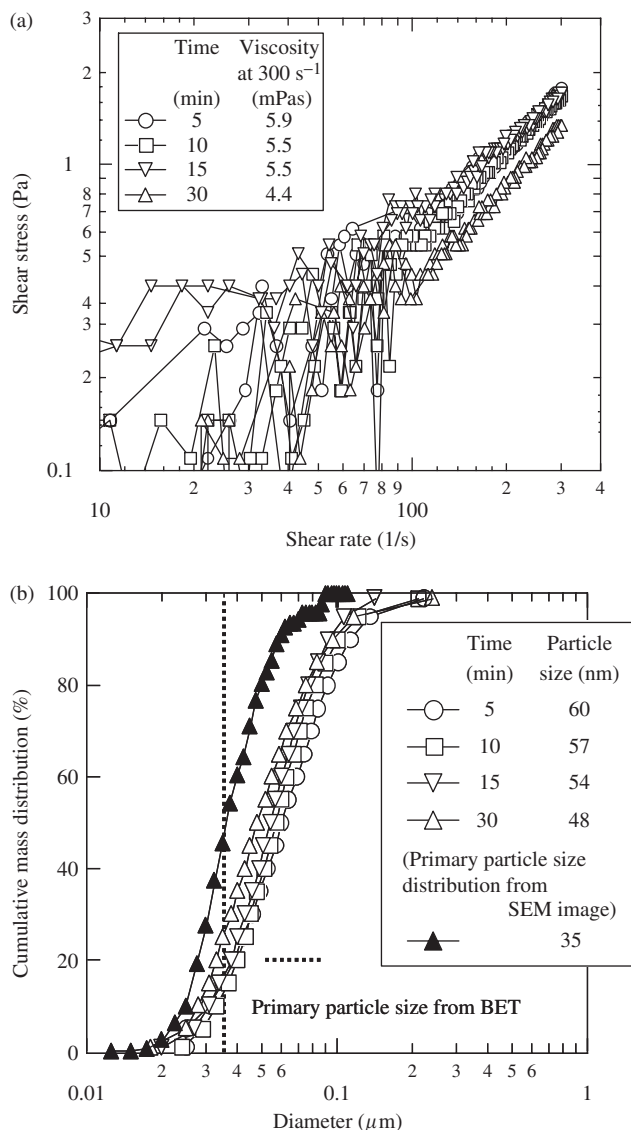

Fig. 4. Zeta potential of TiO₂ nanoparticles (P25 and ST21) at different pHs.

(a)

Time (min)	Viscosity at 300 s^{-1} (mPas)
○ 5	9.6
□ 10	6.0
△ 15	6.2
▽ 30	4.5

(b)

	Time (min)	Particle size (nm)
○	5	69
△	10	62
□	15	55
▽	30	55
(Primary particle size distribution from SEM image)		
▲		35

Primary particle size from BET

Fig. 5. Effect of ultrasonic irradiation time on suspension flow curve (a) and particle size distribution (b) in suspension of nanoparticle P25. Ultrasonic conditions generated by an ultrasonic generator, UT300, with a 26-mm-diameter generation probe were fixed at frequency 20 kHz and power level 70–120 W, which gives a vibration amplitude of 30–34 μm. Solid fraction is 15 vol%. Dashed line indicates primary particle size estimated from specific surface area. The particle size distributions were measured by an X-ray particle analyzer.

(3)   Comparison with Ball Milling

Figure 7 shows the effects of the molecular weight of PAA, dispersion methods, ultrasonic irradiation, and 5-mm-alumina-ball milling on the flow curve of (a) nanometer- and (b) submicrometer-size TiO$_2$ powders. The suspensions were ultrasonically irradiated by the UT300 at a frequency of 20 kHz and a vibration amplitude of 30–34 μm for 30 min. When nanoparticle powder was used (Fig. 7(a)), the ultrasonically irradiated suspensions had significantly lower viscosities than the ball-milled suspensions, regardless of the molecular weight of PAA. The agglomerated nanoparticles were fragmented by ultrasonic irradiation, but it was difficult to disperse the agglomerates by 5-mm-ball milling. The ultrasonically irradiated suspension with a PAA of 1200 g/mol was higher in viscosity than the others. The ball-milled suspensions with PAAs of 2100, 8000, and 15 000 g/mol had lower viscosities than those with molecular weights of 1200 and 30 000 g/mol. Therefore, it seems that a PAA of 1200

(a)

Time (min)	Viscosity at 300 s^{-1} (mPas)
○ 5	5.9
□ 10	5.5
▽ 15	5.5
△ 30	4.4

(b)

|	Time (min)	Particle size (nm)
○	5	60
□	10	57
▽	15	54
△	30	48
(Primary particle size distribution from SEM image)		
▲		35

Primary particle size from BET

Fig. 6. Effect of ultrasonic irradiation time on (a) suspension flow curve and (b) particle size distribution in suspension of nanoparticle P25 with a solid fraction of 15 vol%. Ultrasonic conditions generated by a ultrasonic generator, SMT600, with a 36-mm-diameter generation probe were fixed at frequency 20 kHz and power level 600 W, which gives a vibration amplitude of 40 μm. Dashed line indicates primary particle size estimated from specific surface area. The particle size distributions were measured by an X-ray particle size analyzer.

g/mol cannot form a loop-train structure on the particle surface, and steric repulsion is not effective in either mechanical dispersion method. By using ultrasonic irradiation, a relatively large PAA of 30 000 g/mol can adsorb on the nanoparticle surfaces during ultrasonication, resulting in almost the same flow curve as for a PAA of 8000 and 15 000 g/mol. This suggests that ultrasonic irradiation produced enough particle surface distance by fragmentation of the agglomeration between each particle; therefore, even PAA, which has the largest molecular size in the present work, of 30 000 g/mol in molecular weights, could adsorb on particles without bridge formation. Consequently, the ultrasonically irradiated slurry has lower viscosity.

In contrast, when submicrometer powder was used (Fig. 7(b)), an appreciable change in suspension viscosity was not observed regardless of the molecular weight of the PAA. To test the effect of the mechanical dispersion method on suspension viscosity, a suspension with a PAA of 15 000 g/mol was prepared by ultrasonic irradiation and 5-mm-ball milling. Again, no appreciable difference was observed between the two mechanical dispersion methods.
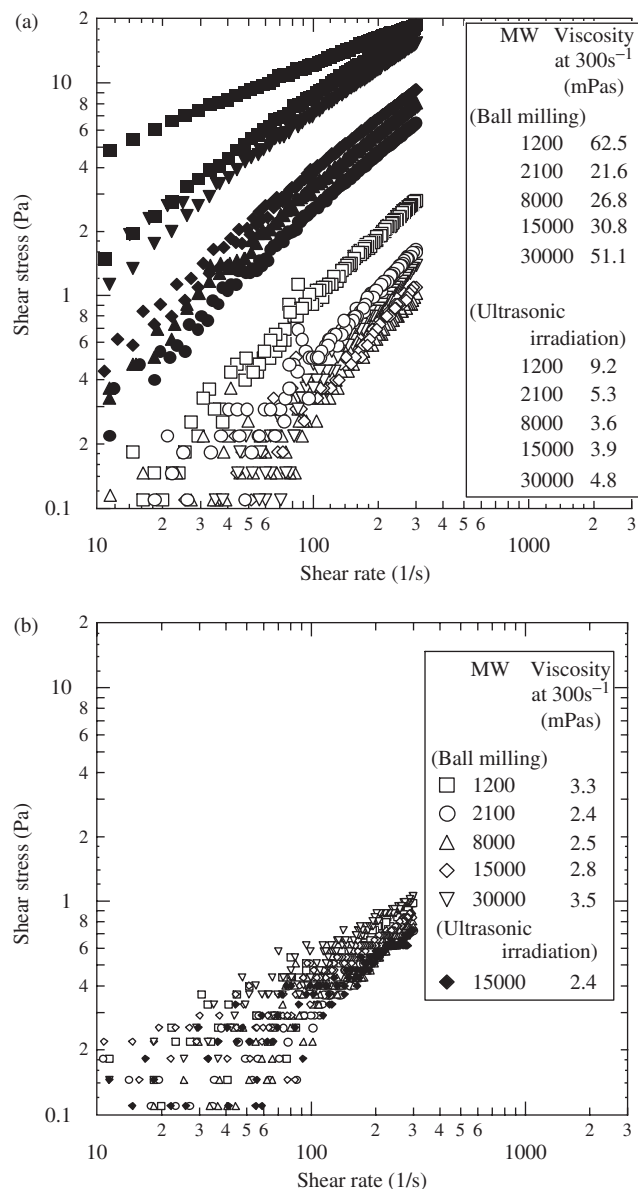
Fig. 7. Effect of molecular weight of PAA on flow curves of suspensions with a solid fraction of 15 vol%. MW denotes molecular weight of PAA. The amount of PAA added was 0.5 mg per unit particle surface area (m^2). (a) P25 (46.5 m^2/g, nanometer sized) suspension. (b) HT0514 (5.8 m^2/g, submicrometer sized) suspension.

Figure 8 shows particle size distributions of the ultrasonically irradiated and ball-milled suspensions for P25 and HT0514. In the submicrometer powder (HT0514) suspension, there is no difference in particle size distribution between the two mechanical dispersion methods. However, the ultrasonically irradiated nanoparticles in the slurry were significantly smaller than the ball-milled ones. The aggregate size distribution of the ultrasonically irradiated nanoparticles approaches that of the primary particle size distribution estimated from the SEM image. It seems that ball milling with 5 mm balls exerts only inhomogeneous and insufficient shear stress on nanoparticles but that ultrasonic irradiation causes homogeneous and frequent collision among nanoparticles. The aggregates of nanoparticles in the suspension were observed to be fragmented and homogeneously dispersed by ultrasonication.

(4) Comparison with Bead Milling

Figure 9 shows the temporal variation in particle size distributions of the suspensions with the volume fraction of 1 vol% prepared by bead milling at two agitation rates. The particle size distributions
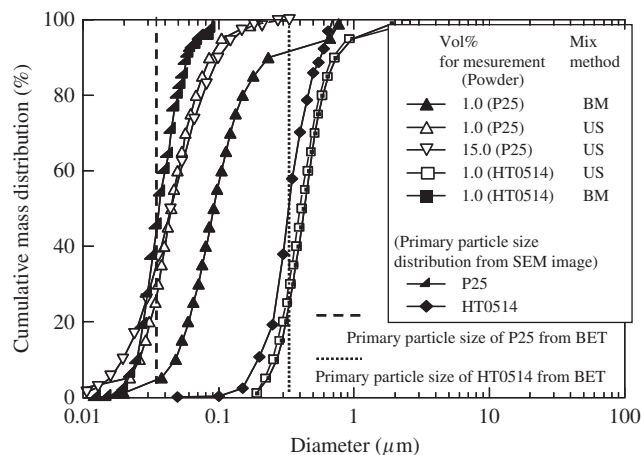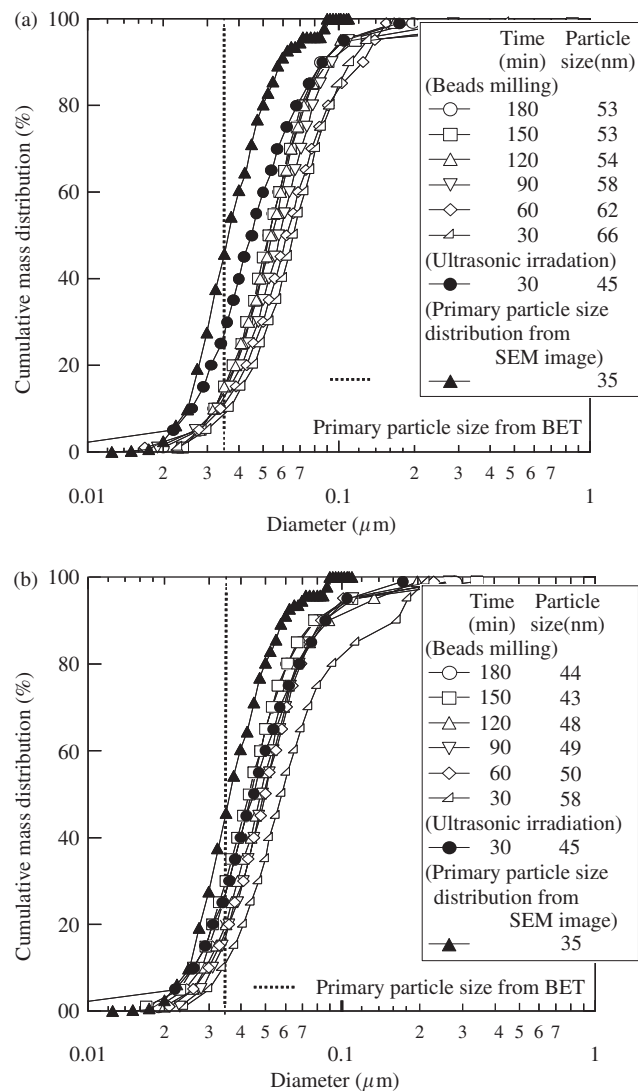

Fig. 8. Particle size distributions in suspensions with a solid fraction of 15 vol% prepared by ultrasonic irradiation and ball milling; d_{50} is the mean particle size. Dotted and dashed lines indicate primary particle sizes estimated from specific surface area of P25 and HT0515, respectively. BM and US denote ball milling and ultrasonic irradiation, respectively. For 15 and 1 vol% suspensions, the particle size distributions were measured by an ultrasonic attenuation spectrometer and an X-ray particle analyzer, respectively.

of the suspensions milled at 4 and 8 m/s are shown in Figs. 9(a) and (b), respectively. The particle size distribution of the suspensions at both agitation rates decreased significantly as milling time increased. The mean particle diameter milled at 4 m/s saturated at 53 nm at a milling time of 120 min, and that milled at 8 m/s saturated at 43 nm at a milling time of 150 min. The mean particle diameter of the bead-milled suspension at 8 m/s for over 150 min was almost the same as that of the suspension with the volume fraction of 15 vol% that was ultrasonically irradiated for 30 min. Because 50-μm-bead milling cannot be applied to the dispersion of dense suspensions with volume fractions higher than 2–3 vol%, ultrasonic irradiation is a useful method in obtaining a highly dispersed dense suspension with a high solid fraction.
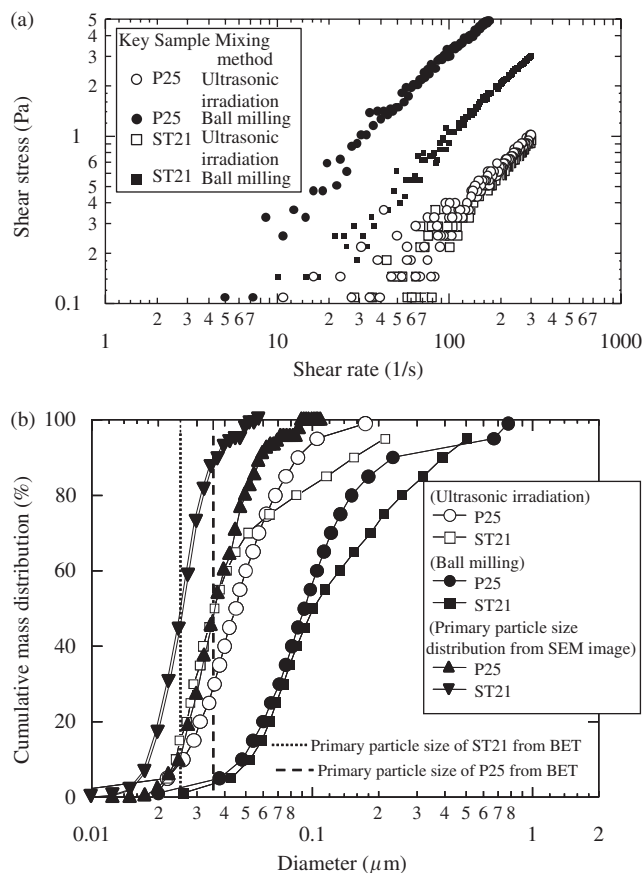
(5) Effects of the Different Starting Materials

To discuss the effects of preparation method of TiO₂ nanoparticles on dispersion behavior in aqueous suspension using different mechanical methods and polymer dispersants, ST21 (63.5 m^2/g specific surface area) was used to prepare suspension. Figures 10(a) and (b) show the flow curve and particle size distributions, respectively, of the P25 and ST21 suspensions prepared with ultrasonic irradiation (20 kHz, 30–34 μm, 70–120 W, 30 min) and ball milling (24 h, 5 mm Al₂O₃ balls). The aggregate size distributions and viscosities of the ultrasonically irradiated nanoparticle suspensions were significantly lower than the ball-milled ones. The ball-milled ST21 suspension had a lower viscosity than the P25 suspension. In contrast, the viscosities of both ultrasonicated suspensions were about the same. The ball-milled and the ultrasonically irradiated ST21 suspensions had much coarser particles than the similarly treated P25 suspensions. Despite the wider aggregate size distribution in the ST21 slurry, the apparent viscosity of the ST21 slurry was lower than that of the P25 slurry. Because of the coagulation of ST21 was stronger than that of P25, the ST21 agglomerated particles were able to act like coarse particles. In the ultrasonically irradiated ST21 suspension, there were a large amount of coarse aggregates of more than 100 nm, and there were also a large amount of small clusters consisting of a few particles of <40 nm. Consequently, the ultrasonically irradiated ST21 suspension had almost the same viscosity as the ultrasonically irradiated P25 slurry. As mentioned above, regardless of the synthesis method, ultrasonication remarkably and more effectively promoted the dispersion of nanoparticles in aqueous suspension than ball milling with 5 mm balls.

Fig. 9. Temporal variation in particle size distributions of nanoparticulate TiO$_2$ suspensions with a solid fraction of 1 vol% prepared by 50-μm-bead milling at agitation times of (a) 4 m/s and (b) 8 m/s. Particle size distributions in suspensions with a solid fraction of 15 vol% prepared by ultrasonic irradiation are included for reference. Dashed line indicates primary particle size estimated from specific surface area. The particle size distributions were measured by an X-ray particle analyzer.

Fig. 10. (a) Flow curves and (b) particle size distributions of P25 (vapor phase synthesis) and ST21 (wet-chemical synthesis) suspensions with a solid fraction of 15 vol%. Dotted and dashed lines in (b) indicate primary particle sizes estimated from specific surface area, respectively, of nanoparticulate ST21 (63.5 m^2/g) and P25 (46.5 m^2/g). The particle size distributions were measured by an X-ray particle analyzer.

IV. Conclusion

The effect of ultrasonic irradiation on viscosity and particle size distribution in aqueous suspensions of submicrometer- and nanometer-scale TiO$_2$ particles was investigated and compared with the effects of ball milling with 5 mm Al$_2$O$_3$ balls and bead milling with 50 μm ZrO$_2$ beads. For submicrometer powders, viscosity and size distribution in the suspension prepared by ultrasonic irradiation were almost the same as those prepared by ball milling. In contrast, for a suspension made of nanometer-sized powders, suspension viscosity and size distribution after ultrasonic irradiation were significantly lower than after ball milling. Aggregate size of the ultrasonically irradiated suspension was close to the primary particle size estimated from the specific surface area in relatively concentrated suspensions of up to 15 vol% solid fraction. The optimum molecular weights of PAA for nanoparticle dispersion by ultrasonication were 8000 or 15 000 g/mol. For suspensions with low volume fractions of nanoparticles, 50-μm-bead milling was able to disperse aggregates of nanoparticles up to primary particles and obtain almost the same size distribution in suspension as ultrasonic irradiation. However, 50-μm-bead milling cannot be applied to concentrated

suspensions. It is concluded that ultrasonic irradiation is a useful way of dispersing nanoparticles in concentrated aqueous suspensions.

References

[1]A. L. Linsebigler, G. Lu, and J. T. Yates, "Photocatalysis on TiO$_2$ Surfaces—Principle, Mechanism, and Selected Results," *Chem. Rev.*, **95**, 735–58 (1995).

[2]A. Hagfeldt and M. Gratzel, "Molecular Photovoltaics," *Acc. Chem. Res.*, **33** [5] 269–77 (2000).

[3]S. Y. Huang, L. Kavan, I. Exnar, and M. J. Gratzel, "Rocking Chair Lithium Battery Based on Nanocrystalline TiO$_2$ (Anatase)," *J. Electrochem. Soc.*, **142** [9] L142–4 (1995).

[4]T. Gerfin, M. Gratzel, and L. Walder, "Molecular and Supramolecular Surface Modification of Nanocrystalline TiO$_2$ Films: Charge-Separating and Charge-Injecting Devices," *Prog. Inorg. Chem.*, **44**, 345–93 (1997).

[5]H. M. Lin, C. H. Keng, and C. Y. Tung, "Hydrogen Sulfide Detection by Nanocrystal PT Doped TiO$_2$-Based Gas Sensors," *Nanostruct. Mater.*, **6**, 5–8, 1001–4 (1995).

[6]S. Vemury and S. E. Pratsinis, "Dopants in Flame Synthesis of Titania," *J. Am. Ceram. Soc.*, **78** [11] 2984–92 (1995).

[7]C. C. Wang and J. Y. Ying, "Sol–Gel Synthesis and Hydrothermal Processing of Anatase and Rutile Titania Nanocrystals," *Chem. Mater.*, **11** [11] 3113–20 (1999).

[8]S. Peres-Durand, J. Rouviere, and C. Cuizard, "Sol–Gel Processing of Titania Using Reverse Micellar Systems as Reaction Media," *Colloids and Surfaces A: Physicochem. Eng. Aspects*, **98** [3] 251–70 (1995).

[9]H. Kamiya, J. Yoneyama, Y. Fukuda, H. Abe, and M. Naito, "Analysis of Anionic Polymer Dispersant in Dense Alumina Suspension with Various Additive Content by Using Colloidal Probe AFM," *Ceram. Trans.*, **133**, 65–70 (2002).

[10]R. Greenwood and K. Kendall, "Selection of Suitable Dispersants for Aqueous Suspensions of Zirconia and Titania Powders Using Acoustophoresis," *J. Eur. Ceram. Soc.*, **19**, 479–88 (1999).

[11]M. Inkyo, T. Tahara, T. Iwaki, F. Iskandar, C.-J. Hogan, Jr., and K. Okuyama, "Investigation of Nanoparticle Dispersion by Beads Centrifugal Bead Separation," *J. Colloid Interface Sci.*, **304**, 535–40 (2006).

[12]O. Hayakawa, K. Nakahira, M. Naito, and J. Tsubaki, "Experimental Analysis of Sample Preparation Conditions for Particle Size Measurement," *Powder Technol.*, **100**, 61–8 (1998).

[13]K. A. Kusters, S. E. Pratsinis, S. G. Thoma, and D. M. Smith, "Energy-Size Reduction Laws for Ultrasonic Fragmentation," *Powder Technol.*, **80**, 253–63 (1994).

[14]S. J. Doktycz and K. S. Suslick, "Interparticle Collisions Driven by Ultrasound," *Science*, **247**, 1067–9 (1990).

[15]S. G. Thoma, M. Ciftcioglu, and D. M. Smith, "Determination of Agglomerate Strength Distributions Part 1. Calibration Via Ultrasonic Forces," *Powder Technol.*, **68**, 53–61 (1991).

[16]K. Higashitani, K. Yoshida, N. Tanise, and H. Murata, "Dispersion of Coagulated Colloids by Ultrasonication," *Colloids Surf. A: Physicochem. Eng. Aspects*, **81**, 167–75 (1993).

[17]S. G. Thoma, M. Ciftcioglu, and D. M. Smith, "Determination of Agglomerate Strength Distributions Part 3. Application to Titania Processing," *Powder Technol.*, **68**, 71–8 (1991).

[18]T. Suzuki, Y. Sakka, K. Nakano, and K. Hiraga, "Effect of Ultrasonication on the Microstructure and Tensile Elongation of Zirconia-Dispersed Alumina Ceramics Prepared by Colloidal Processing," *J. Am. Ceram. Soc.*, **84**, 9, 2132–4 (2001).

[19]C.-S. Lee, J.-S. Lee, and S.-T. Oh, "Dispersion Control Fe₂O₃ Nanoparticles Using a Mixed Type of Mechanical and Ultrasonic Milling," *Mater. Lett.*, **57**, 2643–6 (2003).

[20]M. P. Finnegan, H. Zhang, and J. F. Banfield, "Phase Stability and Transformation in Titania Nanoparticles in Aqueous Solutions Dominated by Surface Energy," *J. Phys. Chem. C*, **111**, 1962–8 (2007).

[21]M. K. Ridley, V. A. Hackley, and M. L. Machesky, "Characterization and Surface-Reactivity of Nanocrystalline Anatase in Aqueous Solutions," *Langumuir*, **22**, 10972–82 (2006).   ☐